Particle clusters settling under gravity in a viscous fluid

Sławomir Alabrudziński,[1] Maria L. Ekiel-Jeżewska,[2] Daniel Chehata-Gómez,[3,a)] and Tomasz A. Kowalewski[2]
[1]*Department of Process Equipment, Warsaw University of Technology, Jachowicza 2/4, 09-402 Płock, Poland*
[2]*Institute of Fundamental Technological Research, Polish Academy of Sciences, Świętokrzyska 21, 00-049 Warsaw, Poland*
[3]*IUSTI, CNRS UMR 6595, Polytech' Marseille, Technopôle de Château-Gombert, 13453 Marseille Cedex 13, France*

(Received 29 December 2008; accepted 1 June 2009; published online 13 July 2009)

Clusters made of a small number of close solid spherical particles at a random configuration, sedimenting through a viscous fluid at small Reynolds number, were experimentally investigated at a short-time scale. The cluster settling velocities were measured and shown to be well approximated by the ensemble-averaged formula derived earlier for the uniform distribution of the point particles inside a spherical volume. It was emphasized that the "effective radius" of this volume in general should be smaller than the actual radius of a cluster made of the spheres, and the relation between both radii was determined. The formula was also shown to account well for the gravitational settling of rigid conglomerates, measured and computed elsewhere. © *2009 American Institute of Physics*. [DOI: 10.1063/1.3168615]

I. INTRODUCTION

The problem of falling suspension droplets is well studied and the interest in this subject dates back to Refs. 1–5. Clouds made of a large number of randomly distributed solid particles settling under gravity close to each other in a viscous fluid evolve in a remarkable way.[4–8] For a long time, most of the particles recirculate and stay together within a single almost spherical blob, which very slowly flattens and forms an expanding torus. Suddenly, the torus starts to destabilize in a cascade of breakups, observed both experimentally and numerically.[5,6,8]

The blob made of a large number of particles sedimenting in a liquid can be approximated as a viscous fluid droplet falling in a less dense fluid, with the interface replaced by a jump in the value of the particle concentration. The basic hydrodynamic description of the spherical system is the same as that formulated by Batchelor[2] for a bubble of a pure liquid rising up in a fluidized bed. Inside a spherical blob, both particle and fluid velocity fields satisfy the Hadamard–Rybczynski formula, with viscosity increased by the entrapped particles. Such a blob evolves in a similar way as a liquid drop made of a heavier fluid.[5]

However, in numerous industrial, biological, and medical applications, it is also of interest to study clusters made of a *small* number of close microparticles settling under gravity in a fluid. Settling velocities of rigid clusters of touching spheres have been evaluated and measured for various regular geometries.[9,10] In general, however, initial configuration of close spheres is random, the particles move with respect to each other, and the cluster has an irregular shape. Most of the previous studies of such clusters with a small number of close particles at random configurations were based on qualitative observations only.[4]

It is obvious that the hydrodynamic description using the Hadamard–Rybczynski formula, defined for continuous phases, cannot elucidate physics of very small clusters of particles because the continuous description becomes totally depreciated if the number of entrapped particles is small. For example, it has been recently shown that even a hundred of particles is not the sufficiently large number for the rapid destabilization of the cluster, always observed for dense-suspension drops made of at least thousands of particles.[8] On the other hand, numerical simulations using discrete description of individual settling particles, including hydrodynamic interactions between their close surfaces is time consuming, and design of accurate numerical algorithms are challenging. Therefore for practical applications, searching for approximate descriptions is a target to help predicting sedimentation velocity when only the blob geometry and physical properties of the fluid are known.

Therefore the goal of this paper is to perform both qualitative and quantitative experimental analyses of groups made of a small number of close particles at a random configuration, falling in a viscous fluid, and to model its settling theoretically. The focus is to investigate motion of the clusters and individual particles at the short-time scale, when the initial distribution of the particles has not been changed too much.

For the uniform N-particle distribution inside a spherical volume of radius R, in the low Reynolds number regime, for the Stokes equations and the point-particle approximation, statistical mechanics has been recently used to derive the ensemble-averaged particle and fluid velocity fields.[7] The following expression for the ensemble-averaged cluster settling velocity has been obtained:

[a)]Also at Faculty of Science and Technology, University of Twente, 7500 AE Enschede, Netherlands.

$$V = U_0\left[1 + \frac{6(N-1)a}{5R}\right], \tag{1}$$

where a is the sphere radius, and U_0 is the Stokes settling velocity of a single sphere.

In this paper, we aim to check if the above point-particle result can be useful for compact clusters of spherical beads close to each other, when the lubrication effects are present. We focus on clusters made of a small number $N \leq 15$ of spherical beads with random initial positions. The settling process is experimentally investigated at the short-time scale. The settling velocity of clusters is measured and compared with the ensemble-averaged relation (1) for the uniform distribution of point particles.

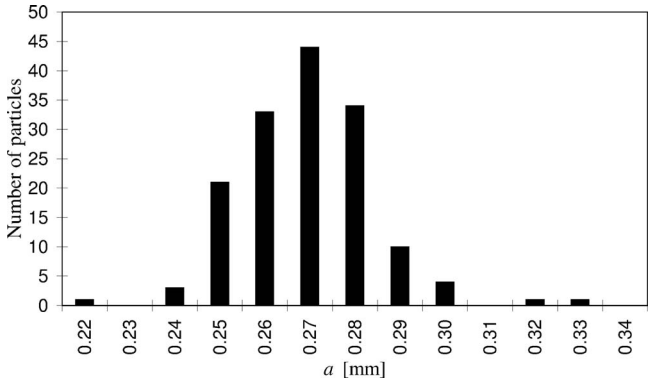

FIG. 1. Distribution of radii of the particles in all the clusters investigated experimentally (measured from the images).

II. EXPERIMENTS

A. Experimental system

Experiments were performed in a glass-wall vessel with an inner cross section of 200×200 mm^2 and a fluid height of 340 mm. To minimize thermal fluctuations, the vessel was inserted in a larger container creating thermal insulation by a gap of air between bottom and sidewalls. In the experiments a 95% glycerin-water mixture (in mass fraction[11]) was used as the ambient fluid. To minimize absorption of water from the air, most of the time the mixture was covered by an insulating cap. The temperature of the fluid inside the vessel was continuously measured with two thermocouples situated near two opposite vertical walls of the container. It was equal to 24.2 °C, with the 0.4 °C variation arising from the temperature change from experiment to experiment. The viscosity of the mixture was measured with a Hoppler KF 10 viscometer within temperatures between 20 and 30 °C (with step 2 °C) and interpolated by an exponential curve.[11] In this range, viscosity changed from 0.265 to 0.579 Pa s. From these measurements, the viscosity at 24.2 °C was $\mu = 0.413 \pm 0.003$ Pa s. The density of the fluid was $\rho_f = 1.23 \pm 0.01$ g cm^{-3}.

The container was backlit by fluorescent bulbs. A diffusive paper sheet was placed between the light bulb and the container to homogenize the illumination. A charge coupled device digital camera (Basler A102F) having a resolution of 1392×1040 pixels was used to record the cluster images with an acquisition rate of 15 frames/s. It was controlled through IEEE1394 interface under Linux operating system. Exposure times less than 6 ms were used. The maximum distance traveled by the clusters during the exposure time was less than a half of the pixel.

The camera was fixed in front of the sedimentation vessel. The measuring section of 39 mm vertical and 29 mm horizontal size was centered at 155 mm from the free surface to avoid wall effects. The minimum distance from the falling clusters to the walls and the free surface was greater than 50 cluster sizes.

Spherical glass particles having a density $\rho_p = 2.51 \pm 0.01$ g cm^{-3} were used. The clusters were prepared by introducing particles one by one onto the tip of a plastic syringe filled with the fluid. A small drop containing all the particles was formed at the tip of the syringe. The drop was released at 20 mm above the free surface. While falling under gravity in a fluid, most of the particles formed a compact cluster. Its motion was registered by the camera. The majority of the clusters kept all the beads together while sedimenting in the fluid, while others lost one or several particles behind. From almost 40 experimental runs, only experiments in which the number of particles in a cluster remained constant and was known exactly during the measurement were analyzed.

Figure 1 shows a monomodal radius distribution of the particles that can be well represented by a mean value and a standard deviation. The mean radius for all the measured particles (nearly 200) was $\langle a \rangle = 0.264$ mm, with a standard deviation $\sigma = 0.015$ mm (5.7% polydispersity).

Due to polydispersity of the beads used in the experiment, higher accuracy was reached when the radius of each particle was measured directly from the camera images. The images with the least overlapping and the best visibility of all particles were chosen. For the specific experiment, the radius of each sphere was measured by circumscribing each particle with a rectangular frame and calculating an average of its height and width. For each cluster, the mean particle radius a was calculated by averaging radii of all the particles at the selected image. The radius uncertainty $\Delta a/a = 2\%-4\%$ was calculated by averaging the uncertainty of a single particle radius determined from the experimental image. For a given experiment, the polydispersity was defined as the ratio of the radius standard deviation to the mean particle radius a. The study was focused on clusters with particle polydispersity less than 10%.

The characteristic Stokes velocity was also calculated separately for each experiment,

$$U_0 = \frac{2g(\rho_p - \rho_f)a^2}{9\mu}, \tag{2}$$

with the viscosity of the mixture of glycerin and water $\mu \equiv \mu(T)$ evaluated for the specific temperature T of the given experiment. For different experiments, U_0 varied from 0.435 to 0.534 mm/s mostly because of the particle polydispersity. Uncertainty of a single measurement of U_0 was evaluated in a standard way using uncertainties of fluid and particle densities, particle radius, and fluid viscosity. ΔU_0 varied from

0.020 to 0.040 mm/s with the largest contribution from the particle radius uncertainty $\Delta a/a$.

For our experimental conditions, the particle Reynolds number was $\mathrm{Re}_p = U_0 a \rho_f / \mu \approx 4 \times 10^{-4}$, and the Stokes number $\mathrm{St} = U_0 a \rho_p / \mu \approx 8 \times 10^{-4}$. We neglect Brownian motion because of the Péclet number, computed as $\mathrm{Pe} = 6\pi\mu U_0 a^2/(k_B T) \approx 6 \times 10^{10}$.

B. Testing experimental conditions

For a uniform fluid viscosity and density, a single particle should have a constant velocity while settling at a low Reynolds number. To test the experimental system, motion of a single sphere far from the container walls was observed. Variations in time of the single sphere settling velocity were investigated. For a single experimental trial, nine images were selected at equal time steps $\Delta t_i = |t_{i+1} - t_i| \approx 15$ s between the beginning and the end of the measurement. At each image, the particle was localized using a circular cursor. The positions in time $[x(t_i), z(t_i)]$ of its center were measured. Successive values of the particle settling velocity were determined as $U_i = [z(t_{i+1}) - z(t_i)]/\Delta t_i$. For a single trial, the differences between U_i were small, with the standard deviation around 1% and $|\max(U_i) - \min(U_i)|/\langle U_i \rangle = 3\%$. The observed velocity variations were consistent with the 3% uncertainty of a single measurement related to the camera resolution. The horizontal component of the particle velocity did not exceed 0.5%.

Insignificant horizontal velocity components measured for the settling single-bead suggested that effects of natural convection in the container can be neglected. To verify this conjecture a particle image velocimetry (PIV) (Ref. 12) technique was used to obtain residual velocity field in the container. For the PIV measurements hollow glass spheres of radius 5 μm were used as a seeding. A light-sheet illumination was introduced, perpendicular to the optical axis of the camera. Two consecutive pictures were taken separated by $\Delta t = 123$ s. The velocity field was evaluated using "in house" developed PIV code. The measured velocity of the tracers did not exceed 0.01 mm/s, which corresponds to less than 2% of the single-bead settling velocity. During these tests the thermal conditions inside container were monitored using four thermocouples situated near vertical walls. The differences between readings from thermocouples were less than 0.2 °C. It was concluded that with the temperature differences ≤ 0.2 °C natural convection can be neglected. Therefore, two of the thermocouples were left in the container during the experiments. The temperature differences between the readings did not exceed 0.2 °C and in this way we ensured that the convection was negligible.

As the last test of the apparatus, 22 spheres were released one by one in separate runs, and values of their settling velocities were measured. The single particle velocity, averaged over all the 22 trials, was equal to 0.505 mm/s, with a standard deviation $\sigma = 0.055$ mm/s. To compare this value with the Stokes formula, the radius of each sphere was measured on one of the images in each trial. The mean calculated Stokes velocity over all the 22 trials was 0.530 mm/s, with the standard deviation $\sigma = 0.058$ mm/s. The 5% differences between measured and calculated particle velocities gave us the upper limit for the experimental accuracy.

III. RESULTS

A. General description of settling clusters

The released clusters settled at a distance of approximately 300 particle diameters until they reached the observation section. Most of the clusters were loosing single particles or groups of particles while settling at irregular time intervals. There were clusters which did not loose any particle for a long time. Therefore we focused on clusters which kept a constant number of particles while being observed by the camera.

The released clusters consisted of $4 \leq N \leq 15$ particles. Vertical sizes of the clusters ranged within two to five particle diameters. The height of the observation section was approximately 80 particle diameters that was over 20 average cluster sizes. These conditions allowed a high accuracy of measuring the particle positions. For each experiment, characteristic properties of the cluster motion are listed in Table I.

A number of clusters seemed to translate with rigid body motion (see Table I). Examples of the corresponding generic cluster shapes are illustrated in Figs. 2 and 3. Nearly symmetric configurations with four and six particles in the cluster (Fig. 2) did not change their shape. Surprisingly, configurations with a "candle-flame" shape also translated almost rigidly, even for a relatively large number of particles (Fig. 3).

However, in most of the clusters with $7 \leq N \leq 15$, the particles were observed to move with respect to each other and the cluster significantly changed its shape. Example of a cluster shape evolution is shown in Fig. 4 and the linked movie.

The change in shape was investigated quantitatively in the following way. On a video image taken at time t, all the particles were enclosed by the smallest possible rectangle with vertical and horizontal sides of length $X(t)$ and $Z(t)$. The center of the cluster was defined as the center of the rectangle. For recirculating clusters, their instantaneous vertical and horizontal sizes, $Z(t)$ and $X(t)$, changed significantly with time. Large fluctuations of the cluster prolateness Z/X were observed during its evolution. An example of such oscillations is shown in Fig. 5. In Ref. 8, prolateness oscillations were also detected numerically on a much longer-time scale, for clusters made of a large number of point particles.

In most of our experiments particles recirculated while settling (see Fig. 4 and Table I) qualitatively in a similar way as fluid inside a drop sedimenting in a lighter fluid or as a symmetrical configuration of spheres, oscillating periodically while settling.[13] The particles located near the center of the cluster moved downward faster than the others. These observations are consistent with previous observations for larger number of particles.[4–8] Also, in many cases, as depicted in Fig. 6, the particle trajectories formed loops, in general, different from the flow lines inside the fluid drop because of coarse-grained hydrodynamic interactions between particles within a small cluster.

TABLE I. The characteristic parameters of the cluster motion—the measurement and the point-particle model given by Eq. (1).

ID	N	Recirculates?	$\langle Z/X\rangle$	λ_0/a	V_e/U_0	Re_c $(\times 10^{-3})$	$R/\langle a\rangle$	V/U_0
24	4	No	1.11	1.9	2.1	1.4	3.83	1.9
25	9	Yes	1.03	3.5	3.0	4.1	4.92	3.0
28	12	Yes	0.98	3.9	3.4	5.1	5.00	3.6
31	14	Yes	0.93	4.0	4.5	5.8	4.94	4.2
32	13	No	1.56	3.8	4.2	5.6	4.78	4.0
34	4	No	0.93	1.9	2.1	1.7	3.77	2.0
38	5	No	1.55	2.1	2.5	1.9	3.72	2.3
39	6	No	1.28	2.3	2.8	2.1	3.67	2.6
41	7	Yes	1.12	2.6	2.7	2.8	3.95	2.8
43	6	No	1.07	1.9	3.0	2.2	2.98	3.0
45	8	Yes	1.61	2.8	3.1	3.7	4.07	3.1
46	10	Yes	1.08	3.5	3.8	5.2	4.69	3.3
48	13	Yes	0.94	4.2	3.4	6.6	5.31	3.7
50	11	No	1.23	3.2	3.9	4.8	4.21	3.8
53	7	Yes	0.76	3.1	2.2	3.0	4.62	2.6
55	8	Yes	0.87	2.8	2.8	3.1	4.07	3.1
57	15	Yes	0.99	4.2	3.8	6.4	5.12	4.3

B. Cluster size, shape, and settling velocity

In our experiments, the time-averaged parameters of the cluster evolution, such as the cluster prolateness, size, and settling velocity, were determined. The averaging was performed for the total observation time (about 20–40 s) over all the observed configurations separated by a time step $\Delta t=1s$. The instantaneous cluster prolateness oscillated with a large amplitude, as shown in Fig. 5. Besides oscillations, during some experiments a small increase or decrease in prolateness Z/X was observed. The averaging time usually exceeded, but not exactly matched, the period of the oscillations. Nevertheless, for most of the recirculating clusters, their average prolateness $\langle Z/X\rangle$ was close to unity. The explicit values of $\langle Z/X\rangle$ are given in Table I. It appears that for the short-time average, most of the clusters had prolateness close to unity and their shape was almost spherical. This observation was similar to the results obtained in Ref. 4 for evolution of initially spherical clouds made of many uniformly distributed point particles—on short-time scales. Such clouds maintained their spherical shape. Therefore, in our experiments a cluster radius was evaluated by averaging an "instantaneous radius" over all the experimental snapshots,

$$\lambda = \langle \sqrt{XZ/\pi} \rangle. \tag{3}$$

The cluster radius relative to the particle radius λ/a varied from 1.9 to 4.2 (see the explicit values in Table I).

The time-averaged cluster settling velocity V_e was determined as the total vertical displacement of the cluster center divided by the total time of its observation. The boost of cluster velocity over the single sphere Stokes velocity was determined as $V_e/U_0=2.1-4.5$, with U_0 calculated from Eq. (2). The explicit values of V_e/U_0 are given in Table I.

The Reynolds number based on the cluster velocity V_e and radius λ was $\mathrm{Re}_c=V_e\lambda\rho_f/\mu$ and was much smaller than unity. For different experiments it varied from 1.5×10^{-3} to 6.6×10^{-3} as shown in Table I.

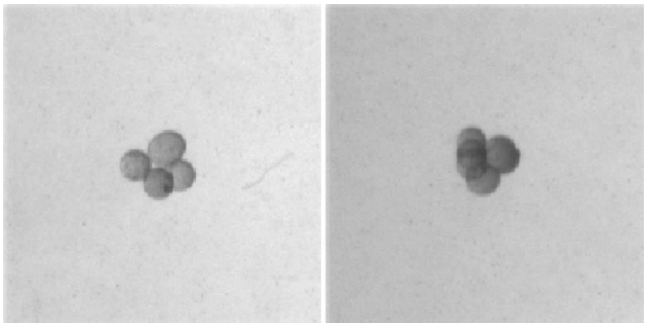

FIG. 2. Clusters with a small even number of particles at an almost symmetric configuration translated as a rigid body (Experiment Nos. 34 and 43 in Table I).

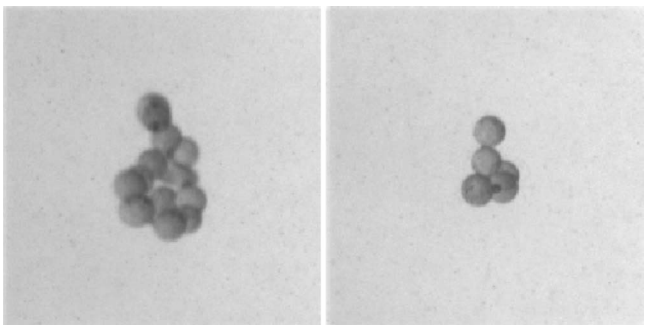

FIG. 3. Particles forming candle-flame configurations translated as a rigid body (Experiment Nos. 32 and 38 in Table I).

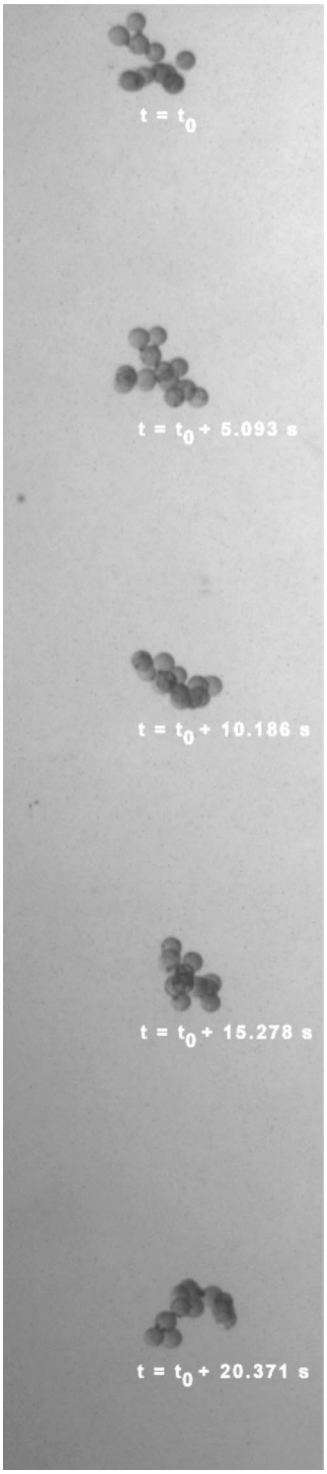

FIG. 4. Detected evolution of a cluster shape (Experiment No. 28 in Table I) (enhanced online).[URL: http://dx.doi.org/10.1063/1.3168615.1]

C. Point-particle model of settling cluster

In a compact cluster, particles are close to each other. Therefore, the mean settling velocity differs from the weight divided by the sum of drag coefficients of isolated particles.[14] To account for the hydrodynamic interactions between the particles we applied the point-particle model.

In the experiments, the initial distribution of the particles inside a drop of the fluid was assumed to be random. Since the evolution was observed at a short-time scale, the particles did not have time to change their distribution significantly. In particular, on the average, the cluster radius λ and the prolateness Z/X did not increase nor decrease systematically during the experiment. Moreover, the time-averaged shape remained almost spherical, with the averaged prolateness close to unity. Therefore it seemed meaningful to compare the measured cluster mean settling velocities V_e with the mean velocity V of a "perfect drop," i.e., the statistical ensemble of clusters made of N particles, distributed with the uniform N-particle probability within a sphere of radius R. Such a result was available within the point-particle approximation.[7] The corresponding expression for the perfect drop of point particles is given in Eq. (1).

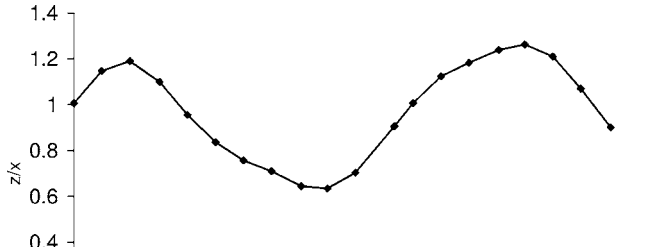

FIG. 5. Example of cluster prolateness Z/X evolution (Experiment No. 28, see Table I).

To compare the measured cluster velocity with the sta-

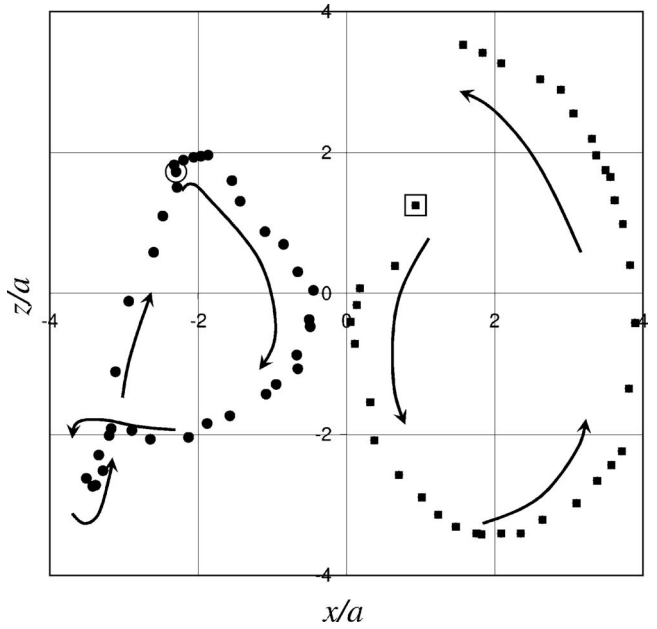

FIG. 6. Exemplary trajectories $[x(t),z(t)]$ of two particles from a cluster which consisted of 14 particles (Experiment No. 31, see Table I). Positions of the particles are plotted relatively to the center of the cluster and scaled by the particle radius a. The initial positions are circumscribed with a square and a circle.

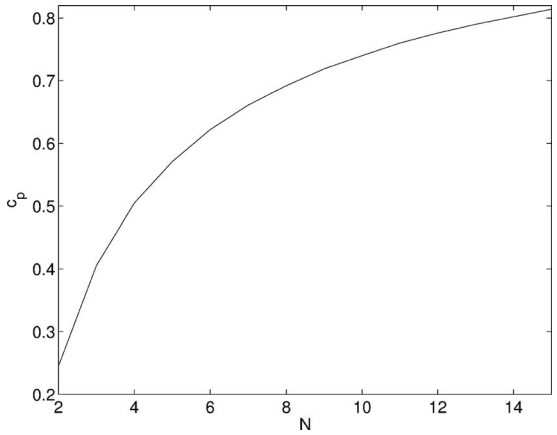

FIG. 7. Correction coefficient c_p for a random point-particle cluster, as defined in Eq. (4).

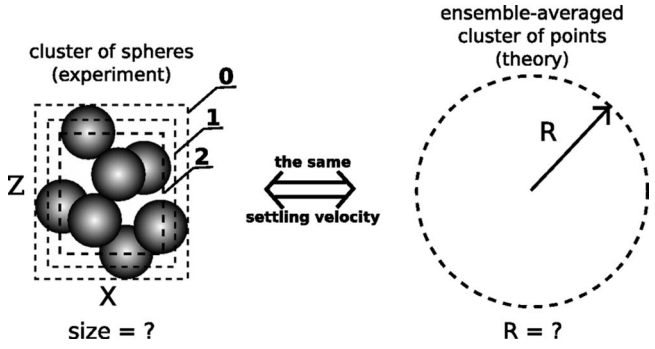

FIG. 8. To apply the point-particle model to the experiment, three effective radii R were tested for three values of ξ, depicted as frames 0, 1, and 2.

tistical formula, it was necessary to relate the radius R of the point-particle ensemble to a time-averaged radius of a given experimental cluster of spheres.

Formula (1) is the ensemble average over random distribution of points inside a sphere of radius R; the radius λ of an individual "drop" [see Eq. (3)] is of course always smaller than R. Therefore, for a given N, we calculated the ensemble-averaged radius c_p of an individual drop, measured in the same way as λ in the experiments, if the point particles are placed at random in a sphere of radius 1. The idea is that one needs to replace λ by λ/c_p. Therefore, 30 000 configurations of $4 \leq N \leq 15$ points were generated at random within the sphere of radius $R=1$, with the uniform N-point probability distribution. For each configuration, the cluster horizontal and vertical dimensions X_p and Z_p were "measured" from the simulations as the maximal horizontal and vertical distances between the points, respectively. Then, the corresponding radius $\sqrt{X_p Z_p/\pi}$ of the cluster of point particles was evaluated and averaged over 30 000 configurations. The result,

$$c_p = \langle \sqrt{X_p Z_p/\pi} \rangle_{30\,000}, \tag{4}$$

in the following called the correction coefficient is plotted in Fig. 7 as a function of the number of the particles N. Naturally, the correction coefficient c_p, as the averaged cluster radius, was smaller than the reference radius $R=1$ of the statistical ensemble. The smaller number of the particles N, the larger the difference. In general, $R \neq 1$; in this case, a cluster average radius is equal to Rc_p, with c_p given by Eq. (4).

To apply the point-particle model to the experiment, we have to take into account the nonzero radius of the spherical particles.[14] Indeed, point particles form a smaller cluster than the real particles, with the cluster radius reduced by the sphere radius a. Moreover, close particle surfaces interact with each other and are not allowed to overlap. The question is how to define such a "corrected" radius λ_0 of a given cluster of spheres that would match the computed radius Rc_p of the cluster of point particles. Should λ_0 be chosen based on positions of the sphere surfaces, of their centers, or else?

We have considered three possibilities to determine the corrected cluster radius λ_0. The first one was to choose λ_0 equal to the cluster radius λ. Another one was to take a much smaller λ_0 calculated from Eq. (3) with X and Z equal to the maximal horizontal and vertical distances between the sphere centers. An intermediate value of λ_0 was also considered. Summarizing, we analyzed three corrected cluster radii,

$$\lambda_0 = \langle \sqrt{(X-\xi a)(Z-\xi a)/\pi} \rangle, \tag{5}$$

with $\xi=0$, 1, and 2. As illustrated in Fig. 8, for each value of ξ, an effective cluster radius (6) was calculated, R,

$$R = \lambda_0/c_p. \tag{6}$$

For each value of $\xi=0$, 1, and 2 the ensemble-averaged velocity V was determined from Eq. (1) and compared to the experimental settling velocity V_e. Analyzing data for all the clusters we concluded that the best agreement between V and V_e was observed for the choice of $\xi=1$, see Ref. 14. Therefore the effective radius

$$R = \langle \sqrt{(X-a)(Z-a)/\pi} \rangle / c_p \tag{7}$$

was chosen as the best estimate. In the following only R defined by Eq. (7) was used. The comparison between the measured and the calculated settling velocities is presented in Fig. 9.[15] The measured cluster settling velocities V_e are depicted relatively to single particle Stokes velocity U_0, which was calculated separately for each cluster from Eq. (2). To calculate U_0 and $6(N-1)a/(5R)$, the mean particle radius a was evaluated separately for each experiment.

The error bars in Fig. 9 were determined separately for each experimental trial. The most significant contribution to error of V_e/U_0 was due to the uncertainty of the mean particle radius a. Radius of each individual particle was measured on the experimental images because of the relatively large polydispersity. The major source of error for the point-particle model $V=6(N-1)a/(5R)$ was the uncertainty of the correction coefficient c_p. The large uncertainty follows from the difference between velocities of the individual clusters and the ensemble-averaged velocity, significant for a small number of particles.

In Fig. 9, the present measurements are compared to the experimental and numerical results obtained for compact regular conglomerates of 2, 3, 5, and 13 spheres in regular compact configurations.[9,10] The measured and evaluated velocities are independent of the conglomerate orientation. The conglomerate "point-particle radius and velocity" were deter-

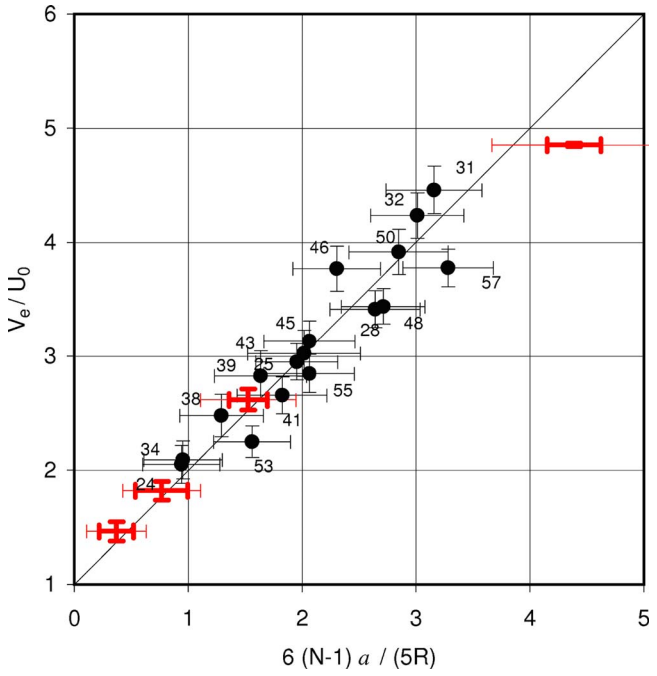

FIG. 9. (Color online) Correlation of the measured cluster settling velocities V_e/U_0 with the ensemble-averaged velocities $6(N-1)a/(5R)$ of point-particle clusters: dots—present results, crosses (red)—experimental and numerical results from Refs. 9 and 10 (superimposed), and straight line—Eq. (1).

mined from Eqs. (7) and (1), for several characteristic orientations, leading to $5.5 \geq R/a \geq 2.3$ and $1.38 \leq V/U_0 \leq 1.55$ for $N=2$, $4.0 \geq R/a \geq 2.3$ and $1.74 \leq V/U_0 \leq 1.900$ for $N=3$ (equilateral triangles), $3.5 \geq R/a \geq 2.8$ and $2.53 \leq V/U_0 \leq 2.71$ for $N=5$, and $3.5 \geq R/a \geq 3.1$ and $4.84 \leq V/U_0 \leq 4.87$ for $N=13$. It is remarkable that for a small number of particles, the settling velocity of rigid conglomerates can be reasonably well approximated by the point-particle statistical formula (1), with the radius given by Eq. (7).

D. Details of the cluster motion

The characteristic parameters of the cluster motion, for all the experiments, are shown in Table I. It contains the measured data and the fitted parameters of the point-particle model. The ID is the successive number of experimental run. The preliminary tests with labels 1–22 were rejected due to insufficient visibility (the frame was too large). Four measurements were eliminated because of bubbles trapped inside the clusters and one because it was not clear how many particles were inside the cluster. From the other 32 runs, only those experiments were selected, which met the criteria of reasonable polydispersity, i.e., less than 10% (three runs were rejected) and the constant number of particles in the cluster during the time of camera registration (11 clusters which lost particles in front of the camera were not analyzed).

The intuitive predictions about parameters, which influence the cluster velocity, are confirmed in Table I. Velocity of the cluster depends on the number of particles N, the cluster radius λ, and also slightly on its prolateness $\langle Z/X \rangle$ (compare Experiment Nos. 45 and 55). In general, the velocity is higher for larger number of particles or smaller cluster size or higher prolateness.

The data listed in Table I and plotted in Fig. 9 confirm that on the average, the velocity V_e of clusters of spheres can be predicted with relatively good agreement using the ensemble-averaged expression (1) for point particles. To achieve the agreement, the effective radius R of the cluster was suitably matched using Eq. (6) with $\xi=1$ (depicted as frame 1 in Fig. 8). The effective radius was greater than the cluster radius λ and the relative difference between them was the smaller the higher values of λ.

IV. CONCLUSIONS

Gravitational settling of a small group of close spherical particles in a viscous fluid was observed experimentally on a short-time scale, corresponding to the cluster displacement not greater than 65 cluster radii λ. In all experiments the Reynolds number based on the cluster velocity and radius was of the order of 5×10^{-3}. Occasionally, individual particles were lost behind the cluster, but most of the particles sedimented together close to each other. Evolution of the clusters was analyzed only when the number of the particles remained unchanged during the measurement time. Some of the clusters, compact and with shape of a special symmetry, fell down rigidly, practically without changing their initial configuration. Particles forming the other clusters recirculated. While evolving, these clusters significantly changed their shape, with large fluctuations or even regular oscillations of the cluster prolateness. In all the experiments, no systematic tendency was observed to increase (or decrease) with time neither the prolateness nor the cluster size. While averaging over time and over many experiments, the apparent cluster shape was almost spherical. This observation served as the motivation to model the cluster sedimentation by a "perfect drop of point particles." It turned out that on the average, the settling velocity of clusters made of spherical particles can be well approximated by the ensemble-averaged velocity of random point-particle clusters, if the cluster effective radius R is appropriately chosen.

For a small group of N close spherical particles, the concept of the effective radius R is essential to achieve the linear relation between the cluster settling velocity and N/R. Note that in the Rotne–Prager approximation, there is no linear scaling, as it was shown in Ref. 16, Fig. 3, for a fixed value of N, different volume fractions (see Fig. 3), and R taken just as the radius of the spherical volume of the cluster. In our experimental study, we would also observe nonlinear deviations from Eq. (1), if we used just the radius λ rather than the effective radius R.

Concluding, in this work the point-particle model[7] was used to propose an empirical statistical formula, Eqs. (1) and (7), for the mean settling velocity of a random cluster of spherical particles sedimenting under gravity. As illustrated in Fig. 9, this relation also approximates well velocity of regular conglomerates of touching spheres, determined experimentally in Ref. 9, and evaluated numerically with a high accuracy in Ref. 10.

ACKNOWLEDGMENTS

Support from CONACyT is gratefully acknowledged by D.C.-G. Both S.A. and M.L.E.-J. thank the COST P21 Action "Physics of droplets" and the Polish Ministry of Science and Higher Education under Grant No. 45/N-COST/2007/0. All the authors benefited from the PAN-CNRS cooperative agreement.

[1] H. C. Brinkman, "A calculation of the viscous force exerted by a flowing fluid on a dense swarm of particles," Appl. Sci. Res., Sect. A **1**, 27 (1949).
[2] G. K. Batchelor, "Low-Reynolds-number bubbles in fluidised beds," Arch. Mech. **26**, 339 (1974).
[3] E. J. Hinch, "Sedimentation of small particles," in *Discorder and Mixing*, edited by E. Guyon, J.-P. Nadal, and Y. Pomeau (Kluwer, Dordrecht, 1988).
[4] J. M. Nitsche and G. K. Batchelor, "Break-up of a falling drop containing dispersed particles," J. Fluid Mech. **340**, 161 (1997).
[5] G. Machu, W. Meile, L. C. Nitsche, and U. Schaflinger, "Coalescence, torus formation and breakup of sedimenting drops: Experiments and computer simulations," J. Fluid Mech. **447**, 299 (2001).
[6] T. Bosse, C. Härtel, E. Meiburg, and L. Kleiser, "Numerical simulation of finite Reynolds number suspension drops settling under gravity," Phys. Fluids **17**, 037101 (2005).
[7] M. L. Ekiel-Jeżewska, B. Metzger, and É. Guazzelli, "Spherical cloud of point particles falling in a viscous fluid," Phys. Fluids **18**, 038104 (2006).
[8] B. Metzger, M. Nicolas, and É. Guazzelli, "Falling clouds of particles in viscous fluids," J. Fluid Mech. **580**, 283 (2007).
[9] I. A. Lasso and P. D. Weidman, "Stokes drag on hollow cylinders and conglomerates," Phys. Fluids **29**, 3921 (1986).
[10] B. Cichocki and K. Hinsen, "Stokes drag on conglomerates of spheres," Phys. Fluids **7**, 285 (1995).
[11] P. N. Shankar and M. Kumar, "Experimental determination of the kinematic viscosity of glycerol-water mixtures," Proc. R. Soc. London, Ser. A **444**, 573 (1994).
[12] M. Raffel, Ch. E. Willert, and J. Kompenhans, *Particle Image Velocimetry: A Practical Guide* (Springer, Berlin, 1998).
[13] R. E. Caflisch, C. Lim, J. H. C. Luke, and A. S. Sangani, "Periodic solutions for three sedimenting spheres," Phys. Fluids **31**, 3175 (1988).
[14] See EPAPS supplementary material at http://dx.doi.org/10.1063/1.3168615 for plots which illustrate the reasoning applied to derive the expression plotted in Fig. 9. In this document, it is shown that intuitive predictions need to be modified to account for the experimental data, and it is explained what are the physical processes responsible for these modifications.
[15] Another method of calculating the cluster radius, alternative to Eq. (3), was also tested, with $\lambda = \langle \sqrt{X^2+Z^2}/2 \rangle$. The corresponding correction coefficient c_p and the cluster corrected radii λ_0 were calculated. However, there was no significant difference in the resulting values of the effective radii R.
[16] G. C. Abade and F. R. Cunha, "Computer simulation of particle aggregates during sedimentation," Comput. Methods Appl. Mech. Eng. **196**, 4597 (2007).